


Motion Detection in Diffraction Tomography

Michael Quellmalz | TU Berlin | RICAM Special Semester Tomography Across the Scales, Workshop Inverse Problems on Small Scales, 20 October 2022
joint work with Robert Beinert, Peter Elbau, Clemens Kirisits, Monika Ritsch-Marte, Otmar Scherzer, Eric Setterqvist, Gabriele Steidl

Content

Optical Diffraction Tomography (ODT)

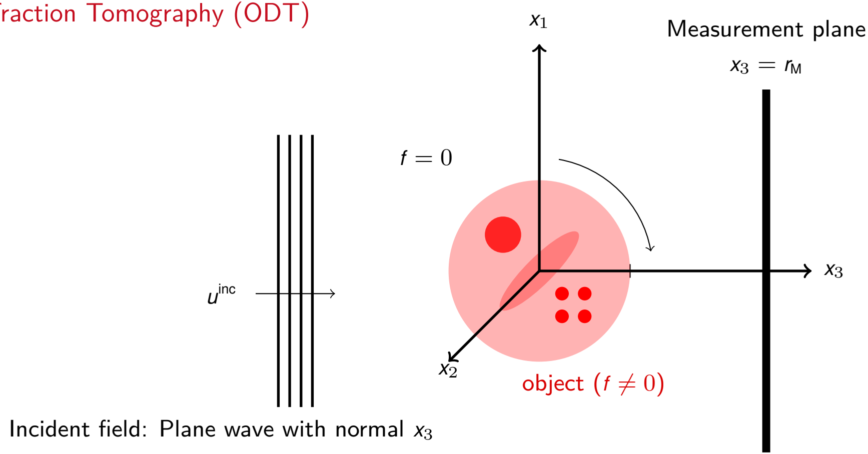

C Kirisits, M Quellmalz, M Ritsch-Marte, O Scherzer, E Setterqvist, G Steidl.
Fourier reconstruction for diffraction tomography of an object rotated into arbitrary orientations.
Inverse Problems 37, 2021.

Optical Diffraction

Optical diffraction occurs when the wavelength of the imaging beam is large $\approx$ the size of the object (μm scale)

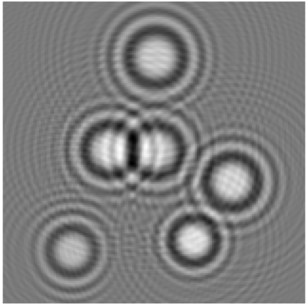

Simulation of the scattered field from spherical particles (size $\approx$ wavelength)

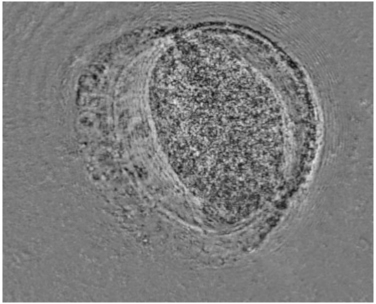

Image with diffraction

Arbitrary rotations

- Sample confinement, such as fixation on a surface or embedding in a gel, has substantial impact on biological cell clusters
- Contact-less tools for 3D manipulation based on optical and acoustical tweezers

  [Kvåle-Løvmo, Pressl, Thalhammer, Ritsch-Marte 2020]
- Drawback: less control about the exact movement

Video of trapped specimen (pollen)

Model of Optical Diffraction Tomography (for one direction)

- We have: field $u^{\text{tot}}(x_1, x_2, r_M)$ at measurement plane $x_3 = r_M$
- We want: scattering potential $f(\boldsymbol{x})$ with $\operatorname{supp} f \subset \mathcal{B}_{r_M} \subset \mathbb{R}^3$
- Object illuminated by plane wave $u^{\text{inc}}(\boldsymbol{x}) = e^{ik_0 x_3}$
- Total field $u^{\text{tot}}(\boldsymbol{x}) = u^{\text{sca}}(\boldsymbol{x}) + u^{\text{inc}}(\boldsymbol{x})$ solves the wave equation

$$-\left(\Delta + f(\boldsymbol{x}) + k_0^2\right) u^{\text{tot}}(\boldsymbol{x}) = 0$$

- Rearranging yields

$$-\left(\Delta + k_0^2\right) u^{\text{sca}}(\boldsymbol{x}) - \underbrace{\left(\Delta + k_0^2\right) u^{\text{inc}}(\boldsymbol{x})}_{=0} = f(\boldsymbol{x}) \left(u^{\text{sca}}(\boldsymbol{x}) + u^{\text{inc}}(\boldsymbol{x})\right)$$

Born approximation

Assuming $|u^{\text{sca}}| \ll |u^{\text{inc}}|$, we obtain

$$-\left(\Delta + k_0^2\right) u^{\text{sca}}(\boldsymbol{x}) = f(\boldsymbol{x}) u^{\text{inc}}(\boldsymbol{x})$$

Model of Optical Diffraction Tomography (for one direction)

- We have: field $u^{\text{tot}}(x_1, x_2, r_{\mathrm{M}})$ at measurement plane $x_3 = r_{\mathrm{M}}$
- We want: scattering potential $f(\boldsymbol{x})$ with $\operatorname{supp} f \subset \mathcal{B}_{r_{\mathrm{M}}} \subset \mathbb{R}^3$
- Object illuminated by plane wave $u^{\text{inc}}(\boldsymbol{x}) = \mathrm{e}^{\mathrm{i}k_0 x_3}$
- Total field $u^{\text{tot}}(\boldsymbol{x}) = u^{\text{sca}}(\boldsymbol{x}) + u^{\text{inc}}(\boldsymbol{x})$ solves the wave equation

$$-\left(\Delta + f(\boldsymbol{x}) + k_0^2\right) u^{\text{tot}}(\boldsymbol{x}) = 0$$

- Rearranging yields

$$-\left(\Delta + k_0^2\right) u^{\text{sca}}(\boldsymbol{x}) - \underbrace{\left(\Delta + k_0^2\right) u^{\text{inc}}(\boldsymbol{x})}_{=0} = f(\boldsymbol{x}) \left(u^{\text{sca}}(\boldsymbol{x}) + u^{\text{inc}}(\boldsymbol{x})\right)$$

Born approximation

Assuming $|u^{\text{sca}}| \ll |u^{\text{inc}}|$, we obtain

$$-\left(\Delta + k_0^2\right) u^{\text{sca}}(\boldsymbol{x}) = f(\boldsymbol{x}) u^{\text{inc}}(\boldsymbol{x})$$

Model of Optical Diffraction Tomography (for one direction)

- We have: field $u^{\text{tot}}(x_1, x_2, r_M)$ at measurement plane $x_3 = r_M$
- We want: scattering potential $f(\boldsymbol{x})$ with $\operatorname{supp} f \subset \mathcal{B}_{r_M} \subset \mathbb{R}^3$
- Object illuminated by plane wave $u^{\text{inc}}(\boldsymbol{x}) = \mathrm{e}^{ik_0 x_3}$
- Total field $u^{\text{tot}}(\boldsymbol{x}) = u^{\text{sca}}(\boldsymbol{x}) + u^{\text{inc}}(\boldsymbol{x})$ solves the wave equation

$$-\left(\Delta + f(\boldsymbol{x}) + k_0^2\right) u^{\text{tot}}(\boldsymbol{x}) = 0$$

- Rearranging yields

$$-\left(\Delta + k_0^2\right) u^{\text{sca}}(\boldsymbol{x}) - \underbrace{\left(\Delta + k_0^2\right) u^{\text{inc}}(\boldsymbol{x})}_{=0} = f(\boldsymbol{x}) \left(u^{\text{sca}}(\boldsymbol{x}) + u^{\text{inc}}(\boldsymbol{x})\right)$$

Born approximation

Assuming $\left|u^{\text{sca}}\right| \ll \left|u^{\text{inc}}\right|$, we obtain

$$-\left(\Delta + k_0^2\right) u^{\text{sca}}(\boldsymbol{x}) = f(\boldsymbol{x}) u^{\text{inc}}(\boldsymbol{x})$$

Fourier diffraction theorem

Let the previous assumptions hold, $f \in L^p(\mathbb{R}^3)$, $p > 1$, and u^{sca} satisfy the Sommerfeld radiation condition (u is an outgoing wave).

Then

$$\sqrt{\frac{2}{\pi}} \kappa \mathrm{i} e^{-\mathrm{i}\kappa r_M} \mathcal{F}_{1,2} \underbrace{u^{\text{sca}}(k_1, k_2, r_M)}_{\text{measurements}} = \mathcal{F} f(\boldsymbol{h}(k_1, k_2)), \quad (k_1, k_2) \in \mathbb{R}^2,$$

where $\boldsymbol{h}(k_1, k_2) := \begin{pmatrix} k_1 \\ k_2 \\ \kappa - k_0 \end{pmatrix}$ and $\kappa := \sqrt{k_0^2 - k_1^2 - k_2^2}$.

based on [Wolf 1969] [Natterer Wuebbeling 2001] [Kak Slaney 2001]
this version from [Kirisits Q. Ritsch-Marte Scherzer Setterqvist Steidl 2021]

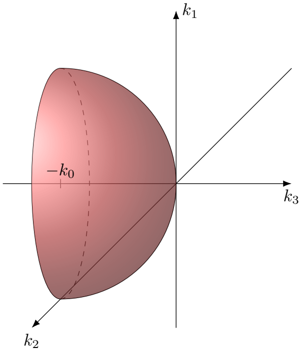

Semisphere $\boldsymbol{h}(\boldsymbol{k})$ of available data in Fourier space

Comparison with Computerized Tomography

Optical diffraction tomography (ODT)

diffraction of imaging wave

Data: Fourier transform on semispheres containing $\mathbf{0}$

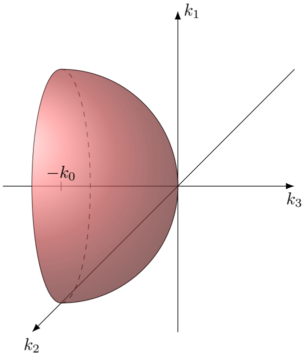

Computerized tomography (CT)

light travels along straight lines

Data: Fourier transform on planes containing $\mathbf{0}$

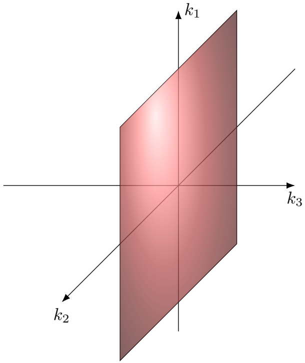

Rigid Motion of the Object

- Scattering potential of the moved object: $f(R_t(\boldsymbol{x} - \boldsymbol{d}_t))$
- Rotation $R_t \in \mathrm{SO}(3)$ (with $R_0 := \mathrm{id}$)
- Translation $\boldsymbol{d}_t \in \mathbb{R}^3$ (with $\boldsymbol{d}_0 := \mathbf{0}$)

Fourier diffraction theorem (with motion)

The quantity

$$\mu_t(k_1, k_2) := \sqrt{\frac{2}{\pi}} \kappa \mathrm{i} \mathrm{e}^{-\mathrm{i}\kappa r_\mathrm{M}} \mathcal{F}_{1,2} \underbrace{u^{\mathrm{sca}}(k_1, k_2, r_\mathrm{M})}_{\text{measurements}} = \mathcal{F} f(R_t \boldsymbol{h}(k_1, k_2))\, \mathrm{e}^{-\mathrm{i}\langle \boldsymbol{d}_t, \boldsymbol{h}(k_1,k_2)\rangle}, \quad \|(k_1, k_2)\| < k_0,$$

depends only on the measurements.

1. Reconstruct the rotation using $\nu_t(k_1, k_2) := |\mu_t(k_1, k_2)|^2 = |\mathcal{F} f(R_t \boldsymbol{h}(k_1, k_2))|^2$.
2. Reconstruct the translation $\boldsymbol{d}_t$
3. Reconstruct f

Rigid Motion of the Object

- Scattering potential of the moved object: $f(R_t(\boldsymbol{x} - \boldsymbol{d}_t))$
- Rotation $R_t \in \mathrm{SO}(3)$ (with $R_0 := \mathrm{id}$)
- Translation $\boldsymbol{d}_t \in \mathbb{R}^3$ (with $\boldsymbol{d}_0 := \mathbf{0}$)

Fourier diffraction theorem (with motion)

The quantity

$$\mu_t(k_1, k_2) := \sqrt{\frac{2}{\pi}} \kappa \mathrm{i} \mathrm{e}^{-\mathrm{i}\kappa r_M} \mathcal{F}_{1,2} \underbrace{u^{\mathrm{sca}}(k_1, k_2, r_M)}_{\text{measurements}} = \mathcal{F} f(R_t \boldsymbol{h}(k_1, k_2)) \, \mathrm{e}^{-\mathrm{i}\langle \boldsymbol{d}_t, \boldsymbol{h}(k_1,k_2)\rangle}, \quad \|(k_1, k_2)\| < k_0,$$

depends only on the measurements.

1. Reconstruct the rotation using $\nu_t(k_1, k_2) := |\mu_t(k_1, k_2)|^2 = |\mathcal{F} f(R_t \boldsymbol{h}(k_1, k_2))|^2$.
2. Reconstruct the translation $\boldsymbol{d}_t$
3. Reconstruct f

Content

Discretization

- Object $f(\boldsymbol{x}_{\boldsymbol{k}})$ with $\boldsymbol{x}_{\boldsymbol{k}} = \boldsymbol{k}\frac{2L_s}{K}$, $\boldsymbol{k} \in \mathcal{I}_K^3 := \{-K/2, \dots, K/2-1\}^3$
- Measurements $u_{t_m}^{\mathrm{tot}}(\boldsymbol{y}_{\boldsymbol{n}}, r_M)$ with $\boldsymbol{y}_{\boldsymbol{n}} = \boldsymbol{n}\frac{2L_M}{N}$, $\boldsymbol{n} \in \mathcal{I}_N^2$
- discrete Fourier transform (DFT)

$$\left[\boldsymbol{F}_{\mathrm{DFT}}\, u_{t_m}^{\mathrm{sca}}\right]_{\boldsymbol{\ell}} := \sum_{\boldsymbol{n}\in\mathcal{I}_N^2} u_{t_m}^{\mathrm{sca}}(\boldsymbol{y}_{\boldsymbol{n}}, r_M)\, \mathrm{e}^{-2\pi \mathrm{i} \boldsymbol{n}\cdot\boldsymbol{\ell}/N}, \qquad \boldsymbol{\ell} \in \mathcal{I}_N^2,$$

- Non-uniform discrete Fourier transform (NDFT)

$$\left[\boldsymbol{F}_{\mathrm{NDFT}}\boldsymbol{f}\right]_{m,\boldsymbol{\ell}} := \sum_{\boldsymbol{k}\in\mathcal{I}_K^3} f_{\boldsymbol{k}}\, \mathrm{e}^{-\mathrm{i}\boldsymbol{x}_{\boldsymbol{k}}\cdot\left(R_{t_m}\boldsymbol{h}(\boldsymbol{y}_{\boldsymbol{\ell}})\right)}, \qquad m \in \mathcal{J}_M,\ \boldsymbol{\ell} \in \mathcal{I}_N^2$$

Discretized forward operator

$$\boldsymbol{D}^{\mathrm{tot}}\boldsymbol{f} := \boldsymbol{F}_{\mathrm{DFT}}^{-1}(\boldsymbol{c} \odot \boldsymbol{F}_{\mathrm{NDFT}}\boldsymbol{f}) + \mathrm{e}^{\mathrm{i}k_0 r_M}, \qquad \boldsymbol{f} \in \mathbb{R}^{K^d},$$

where $\boldsymbol{c} = \left[\frac{\mathrm{i}}{\kappa(\boldsymbol{y}_{\boldsymbol{\ell}})}\, \mathrm{e}^{\mathrm{i}\,\kappa(\boldsymbol{y}_{\boldsymbol{\ell}})\, r_M} \left(\frac{N}{L_M}\right)^{d-1} \left(\frac{L_s}{K}\right)^{d}\right]_{\boldsymbol{\ell}\in\mathcal{I}_N^2}$

Reconstruction of f

Inverse

$$\boldsymbol{f} \approx \boldsymbol{F}_{\mathrm{NDFT}}^{-1}\Big(\big(\boldsymbol{F}_{\mathrm{DFT}}\boldsymbol{u}^{\mathrm{tot}} - \mathrm{e}^{ik_0 r_{\mathrm{M}}}\big) \oslash \boldsymbol{c}\Big)$$

Crucial part: inversion of NDFT $\boldsymbol{F}_{\mathrm{NDFT}}^{-1}$

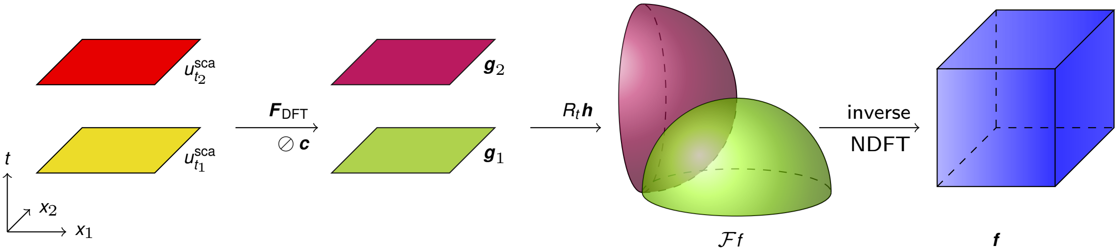

Approach 1: Filtered Backpropagation

Idea: Compute inverse Fourier transform of $\mathcal{F}f$ restricted to the set of available data $\mathcal{Y}$:

$$f_{\mathrm{bp}}(\boldsymbol{x}) := (2\pi)^{-\frac{3}{2}} \int_{\mathcal{Y}} \mathcal{F}f(\boldsymbol{y})\, \mathrm{e}^{\mathrm{i}\boldsymbol{y}\cdot\boldsymbol{x}}\, \mathrm{d}\boldsymbol{y}.$$

Theorem [Kirisits, Q, Ritsch-Marte, Scherzer, Setterqvist, Steidl 2021]

Consider the rotation R_t round axis $\boldsymbol{a}(t)$ with angle $\alpha(t)$ in $C^1[0,T]$. Then

$$f_{\mathrm{bp}}(\boldsymbol{x}) = (2\pi)^{-\frac{3}{2}} \int_0^T \int_{\mathcal{B}_{k_0}} \mathcal{F}f(R_t\boldsymbol{h}(k_1,k_2))\, \mathrm{e}^{\mathrm{i}\,R_t\boldsymbol{h}(k_1,k_2)\cdot\boldsymbol{x}} \frac{|\det \nabla T(k_1,k_2,t)|}{\mathrm{Card}\, T^{-1}(T(k_1,k_2,t))}\, \mathrm{d}(k_1,k_2)\, \mathrm{d}t,$$

where $T(k_1,k_2,t) := R_t\boldsymbol{h}(k_1,k_2)$ and

$$|\det \nabla T(k_1,k_2,t)| = \frac{k_0}{\kappa} \left| \left((1-\cos\alpha)(a_3\,\boldsymbol{a}'\cdot\boldsymbol{h} - a_3'\boldsymbol{a}\cdot\boldsymbol{h}) - a_3\,\boldsymbol{a}\cdot(\boldsymbol{a}'\times\boldsymbol{h})\sin\alpha\right) - \alpha'\,(a_1k_2 - a_2k_1) + (\boldsymbol{a}\cdot\boldsymbol{h})(a_1a_2' - a_2a_1')\sin\alpha \right|.$$

Previously known only for constant axis $\boldsymbol{a}$ [Devaney 1982]

Approach 1: Filtered Backpropagation

Idea: Compute inverse Fourier transform of $\mathcal{F}f$ restricted to the set of available data $\mathcal{Y}$:

$$f_{\mathrm{bp}}(\boldsymbol{x}) := (2\pi)^{-\frac{3}{2}} \int_{\mathcal{Y}} \mathcal{F}f(\boldsymbol{y})\, \mathrm{e}^{\mathrm{i}\boldsymbol{y}\cdot\boldsymbol{x}}\, \mathrm{d}\boldsymbol{y}.$$

Theorem [Kirisits, Q, Ritsch-Marte, Scherzer, Setterqvist, Steidl 2021]

Consider the rotation R_t round axis $\boldsymbol{a}(t)$ with angle $\alpha(t)$ in $C^1[0,T]$. Then

$$f_{\mathrm{bp}}(\boldsymbol{x}) = (2\pi)^{-\frac{3}{2}} \int_0^T \int_{\mathcal{B}_{k_0}} \mathcal{F}f(R_t\boldsymbol{h}(k_1,k_2))\, \mathrm{e}^{\mathrm{i}\,R_t\boldsymbol{h}(k_1,k_2)\cdot\boldsymbol{x}}\, \frac{|\det \nabla T(k_1,k_2,t)|}{\mathrm{Card}\, T^{-1}(T(k_1,k_2,t))}\, \mathrm{d}(k_1,k_2)\, \mathrm{d}t,$$

where $T(k_1,k_2,t) := R_t\boldsymbol{h}(k_1,k_2)$ and

$$|\det \nabla T(k_1,k_2,t)| = \frac{k_0}{\kappa} \left|\big((1-\cos\alpha)(a_3\,\boldsymbol{a}'\cdot\boldsymbol{h} - a_3'\boldsymbol{a}\cdot\boldsymbol{h}) - a_3\,\boldsymbol{a}\cdot(\boldsymbol{a}'\times\boldsymbol{h})\sin\alpha\big) - \alpha'\,(a_1k_2 - a_2k_1) + (\boldsymbol{a}\cdot\boldsymbol{h})(a_1a_2' - a_2a_1')\sin\alpha\right|.$$

Previously known only for constant axis $\boldsymbol{a}$ [Devaney 1982]

Example: Rotation Around the First Axis

[Devaney 1982]

Backpropagation formula $f_{\mathrm{bp}}(\boldsymbol{x}) = (2\pi)^{-\frac{3}{2}} \int_0^T \int_{\mathcal{B}_{k_0}} \mathcal{F}f(R_t\boldsymbol{h}(k_1,k_2))\, \mathrm{e}^{\mathrm{i}\, R_t\boldsymbol{h}(k_1,k_2)\cdot\boldsymbol{x}}\, \frac{k_0\,|k_2|}{2\kappa}\, \mathrm{d}(k_1,k_2)\,\mathrm{d}t$

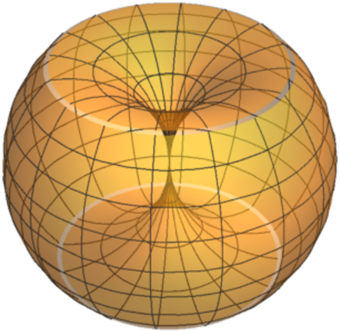

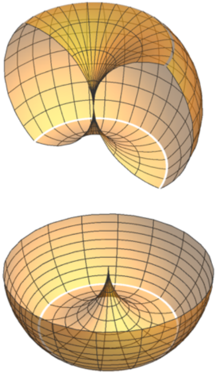

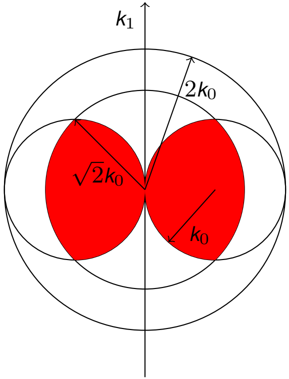

Set $\mathcal{Y}$ of available data in Fourier space

Approach 2: Conjugate Gradient (CG) Method

- Conjugate Gradients (CG) on the normal equations

$$\operatorname*{arg\,min}_{\boldsymbol{f}\in\mathbb{R}^{K^3}} \quad \left\|\boldsymbol{F}_{\mathrm{NDFT}}(\boldsymbol{f}) - \boldsymbol{g}\right\|_2^2$$

- NFFT (Non-uniform fast Fourier transform) for computing $\boldsymbol{F}_{\mathrm{NDFT}}(\boldsymbol{f})$ in $\mathcal{O}\left(N^3 \log N\right)$ steps

[Dutt Rokhlin 93], [Beylkin 95], [Potts Steidl Tasche 01], [Potts Kunis Keiner 04+]

Approach 3: TV (Total Variation) Regularization

- Regularized inverse

$$\operatorname*{arg\,min}_{\boldsymbol{f}\in\mathbb{R}^{K^3}} \quad \chi_{\mathbb{R}^{K^3}_{\geq 0}}(\boldsymbol{f}) + \tfrac{1}{2}\left\|\boldsymbol{F}_{\mathrm{NDFT}}(\boldsymbol{f}) - \boldsymbol{g}\right\|_2^2 + \lambda \mathrm{TV}(\boldsymbol{f}),$$

- Primal-dual (PD) iteration [Chambolle & Pock 2010]
- Adaptive selection of step sizes [Yokota & Hontani 2017]

Approach 2: Conjugate Gradient (CG) Method

- Conjugate Gradients (CG) on the normal equations

$$\operatorname*{arg\,min}_{\boldsymbol{f}\in\mathbb{R}^{K^3}} \quad \|\boldsymbol{F}_{\mathsf{NDFT}}(\boldsymbol{f}) - \boldsymbol{g}\|_2^2$$

- NFFT (Non-uniform fast Fourier transform) for computing $\boldsymbol{F}_{\mathsf{NDFT}}(\boldsymbol{f})$ in $\mathcal{O}\left(N^3 \log N\right)$ steps

[Dutt Rokhlin 93], [Beylkin 95], [Potts Steidl Tasche 01], [Potts Kunis Keiner 04+]

Approach 3: TV (Total Variation) Regularization

- Regularized inverse

$$\operatorname*{arg\,min}_{\boldsymbol{f}\in\mathbb{R}^{K^3}} \quad \chi_{\mathbb{R}^{K^3}_{\geq 0}}(\boldsymbol{f}) + \frac{1}{2}\|\boldsymbol{F}_{\mathsf{NDFT}}(\boldsymbol{f}) - \boldsymbol{g}\|_2^2 + \lambda \mathsf{TV}(\boldsymbol{f}),$$

- Primal-dual (PD) iteration [Chambolle & Pock 2010]
- Adaptive selection of step sizes [Yokota & Hontani 2017]

Test Setup

- Normalized wavelength $1 \Rightarrow k_0 = 2\pi$
- Test function *f* given analytically
- Simulate data via convolution with the Green function (also based on Born approximation) to avoid the "inverse crime"
- "missing cones" around the axis of rotation

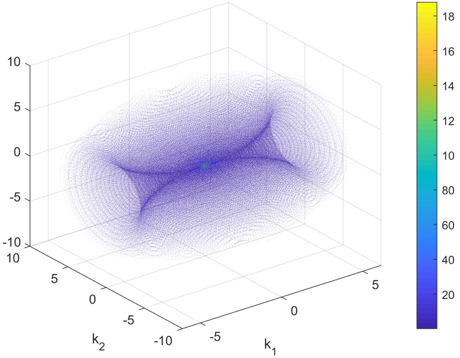

Simulated data: Fourier transform $|\mathcal{F}f|$ at 496944 nodes (constant rotation axis)

Reconstruction: Moving Axis

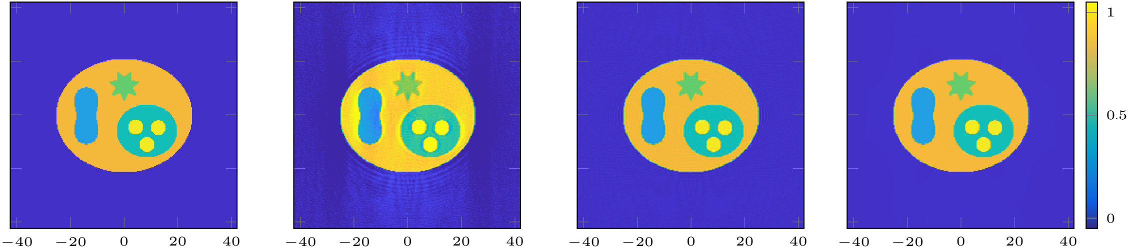

Ground truth $\boldsymbol{f}$
($240 \times 240 \times 240$ grid)

Backpropagation
PSNR 24.17, SSIM 0.171

CG Reconstruction
PSNR 35.84, SSIM 0.962

PD with TV ($\lambda = 0.02$)
PSNR 40.95, SSIM 0.972

R Beinert, M Quellmalz.
Total Variation-Based Reconstruction and Phase Retrieval for Diffraction Tomography with an Arbitrarily Moving Object.
Arxiv preprint 2210.03495

Reconstruction: Moving Axis and 5 % Gaussian Noise

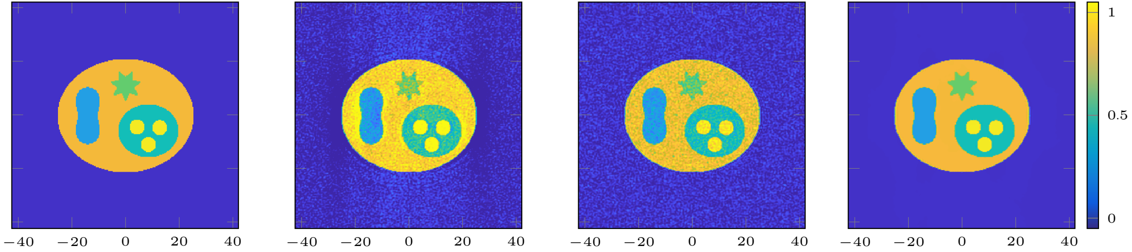

Ground truth $\boldsymbol{f}$

Backpropagation
PSNR 21.19, SSIM 0.075

CG Reconstruction
PSNR 24.10, SSIM 0.193

PD with TV ($\lambda = 0.05$)
PSNR 38.01, SSIM 0.772

Content

Formal Uniqueness Result

Theorem [Kurlberg Zickert 2021]

Let

- the matrix of second-order moments of f have distinct, real eigenvalues,
- certain third-order moments do not vanish,
- the translation $\boldsymbol{d}_t$ be restricted to a known plane,
- the rotations R_t cover $\mathrm{SO}(3)$.

Then f is uniquely determined given the diffraction images u_t for all (unknown) motions.

Our goal: Find an algorithm to recover the rotations and translations

Detection of the Rotation

Goal: Estimate the rotation R_t from the transformed measurements $\nu_t(\boldsymbol{k}) = |\mathcal{F}f(R_t\boldsymbol{h}(\boldsymbol{k}))|^2$

Common circle approach:

- For each t we have the Fourier data $\mathcal{F}f$ on one semisphere
- Two semispheres intersect in a circle (arc), where $\mathcal{F}f$ must agree
- Find the common circle of two semispheres

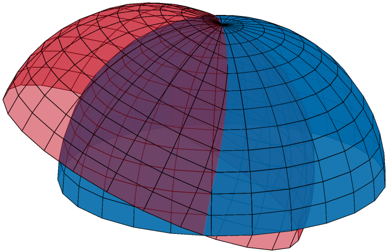

P Elbau, M Quellmalz, O Scherzer, G Steidl.
Motion detection in diffraction tomography with common circle methods.
Arxiv preprint 2209.08086

Common Circles

Theorem [Q. Elbau Scherzer Steidl 2022]

Let $t, s \in [0, T]$ such that there uniquely exist two curves

$$\gamma_{s,t}(\beta) = \frac{k_0}{2} \sin\theta \, (\cos\beta - 1) \begin{pmatrix} \cos\varphi \\ \sin\varphi \end{pmatrix} + k_0 \cos\frac{\theta}{2} \sin\beta \begin{pmatrix} -\sin\varphi \\ \cos\varphi \end{pmatrix}$$

$$\gamma_{t,s}(\beta) = \frac{k_0}{2} \sin\theta \, (\cos\beta - 1) \begin{pmatrix} -\cos\psi \\ \sin\psi \end{pmatrix} + k_0 \cos\frac{\theta}{2} \sin\beta \begin{pmatrix} -\sin\varphi \\ -\cos\varphi \end{pmatrix}$$

with some parameters $\varphi, \psi \in \mathbb{R}/(2\pi\mathbb{Z})$, $\theta \in [0, \pi]$ such that

$$\nu_s \circ \gamma_{s,t}(\beta) = \nu_t \circ \gamma_{t,s}(-\beta), \qquad |\beta| < \pi.$$

Then the rotation $R_s^\top R_t$ has the Euler angles φ, θ, ψ.

Dual Common Circles

- f real-valued (no absorption)
- Additional symmetry $\mathcal{F}f(\boldsymbol{y}) = \overline{\mathcal{F}f(-\boldsymbol{y})}$
- Additional pair of dual common circles

$$\check{\gamma}_{s,t}(\beta) = -\frac{k_0}{2}\sin\theta\,(\cos\beta - 1)\begin{pmatrix}\cos\varphi\\ \sin\varphi\end{pmatrix} + k_0 \sin\frac{\theta}{2}\sin\beta\begin{pmatrix}-\sin\varphi\\ \cos\varphi\end{pmatrix}$$

$$\check{\gamma}_{t,s}(\beta) = -\frac{k_0}{2}\sin\theta\,(\cos\beta - 1)\begin{pmatrix}-\cos\psi\\ \sin\psi\end{pmatrix} + k_0 \sin\frac{\theta}{2}\sin\beta\begin{pmatrix}-\sin\varphi\\ -\cos\varphi\end{pmatrix}$$

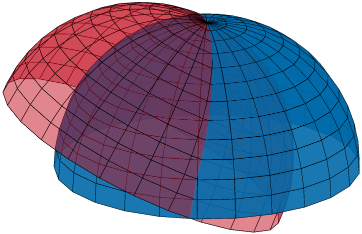

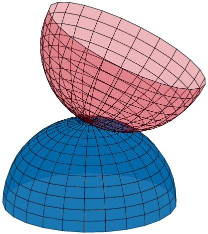

Visualization of the Arcs

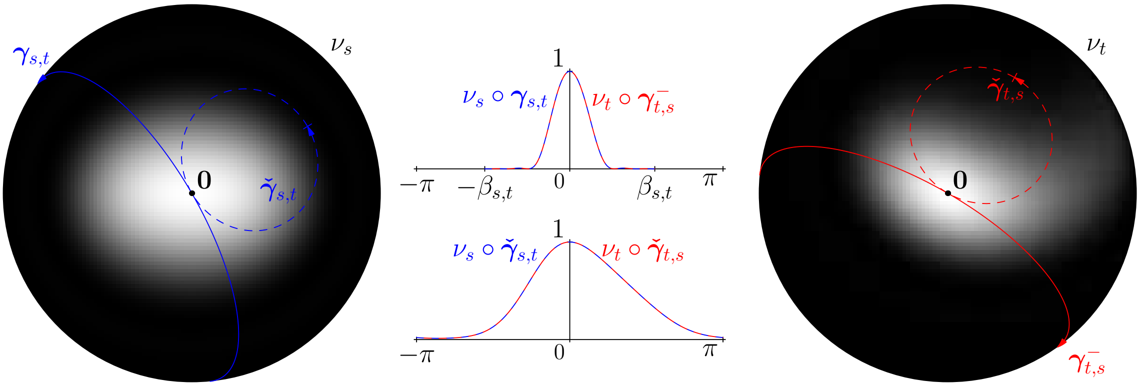

Infinitesimal Common Circles Method

Theorem [Q. Elbau Scherzer Steidl 2022]

Let the rotation $R \in C^1([0,T] \to \mathrm{SO}(3))$ and $t \in (0,T)$.
We define the associated **angular velocity** as the vector $\boldsymbol{\omega}_t \in \mathbb{R}^3$ satisfying

$$R_t^\top R_t' \boldsymbol{y} = \boldsymbol{\omega}_t \times \boldsymbol{y}, \qquad \boldsymbol{y} \in \mathbb{R}^3.$$

and write it in cylinder coordinates

$$\boldsymbol{\omega}_t = \begin{pmatrix} \rho_t \boldsymbol{\varphi}_t \\ \zeta_t \end{pmatrix}, \qquad \boldsymbol{\varphi}_t = \begin{pmatrix} \cos \varphi_t \\ \sin \varphi_t \end{pmatrix} \in \mathbb{S}^1,$$

Then, for all $r \in (-k_0, k_0)$, it holds that

$$-\partial_t \nu_t(r\boldsymbol{\varphi}_t) = \left(\rho(t)\left(\sqrt{k_0^2 - r^2} - k_0\right) + r\zeta_t\right)\left\langle \nabla \nu_t(r\boldsymbol{\varphi}_t), \begin{pmatrix} -\sin \varphi_t \\ \cos \varphi_t \end{pmatrix}\right\rangle.$$

Reconstructing the Translation

Recall: Data $\mu_t(k_1, k_2) = \mathcal{F}f(R_t\boldsymbol{h}(k_1, k_2))\,\mathrm{e}^{-\mathrm{i}\langle \boldsymbol{d}_t, \boldsymbol{h}(k_1,k_2)\rangle}$

Theorem [Q. Elbau Scherzer Steidl 2022]

Let $s, t \in [0, T]$ be such that $R_s\boldsymbol{e}^3 \neq \pm R_t\boldsymbol{e}^3$ and let $f \geq 0$ with $f \not\equiv 0$.
If $\boldsymbol{d}_0 = \mathbf{0}$, then $\boldsymbol{d}_t$ can be uniquely reconstructed from the two equations:

$$\mathrm{e}^{\mathrm{i}\langle R_t\boldsymbol{d}_t - R_s\boldsymbol{d}_s, \boldsymbol{\sigma}_{s,t}(\beta)\rangle} = \frac{\mu_s(\gamma_{s,t}(\beta))}{\mu_t(\gamma_{t,s}(-\beta))}, \qquad \beta \in [-\pi, \pi],\ \mu_s(\gamma_{s,t}(\beta)) \neq 0,$$

and

$$\mathrm{e}^{\mathrm{i}\langle R_t\boldsymbol{d}_t - R_s\boldsymbol{d}_s, \check{\boldsymbol{\sigma}}_{s,t}(\beta)\rangle} = \frac{\mu_s(\check{\gamma}_{s,t}(\beta))}{\overline{\mu_t(\check{\gamma}_{t,s}(\beta))}}, \qquad \beta \in [-\pi, \pi],\ \mu_s(\check{\gamma}_{s,t}(\beta)) \neq 0.$$

Similar reconstruction result for $R_s\boldsymbol{e}^3 = \pm R_t\boldsymbol{e}^3$

Comparision with CT

Method of common lines in Cryo-EM [Crowther DeRosier Klug 70] [van Heel 87] [Goncharov 88] [Wang Singer Zen 13]

- Based on different model (ray transform)
- Requires 3 common planes (instead of 2 semi-spheres)
- Ambiguities (mirroring, translation along imaging direction)

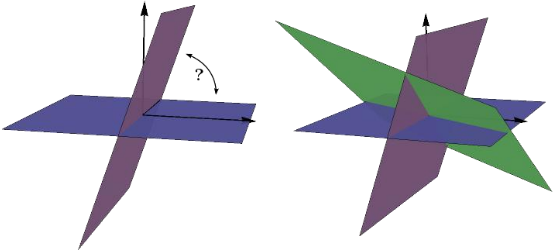

Images by [Schmutz 17]

Numerical Simulation: Test Functions (3D)

Cell phantom

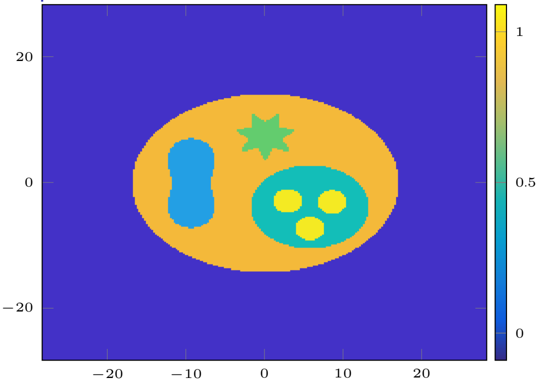

Shepp-Logan phantom

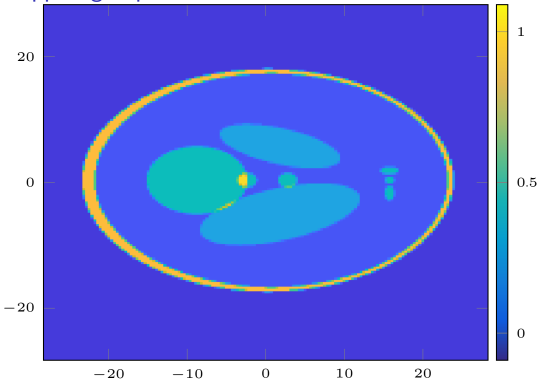

Numerical Simulation: Results

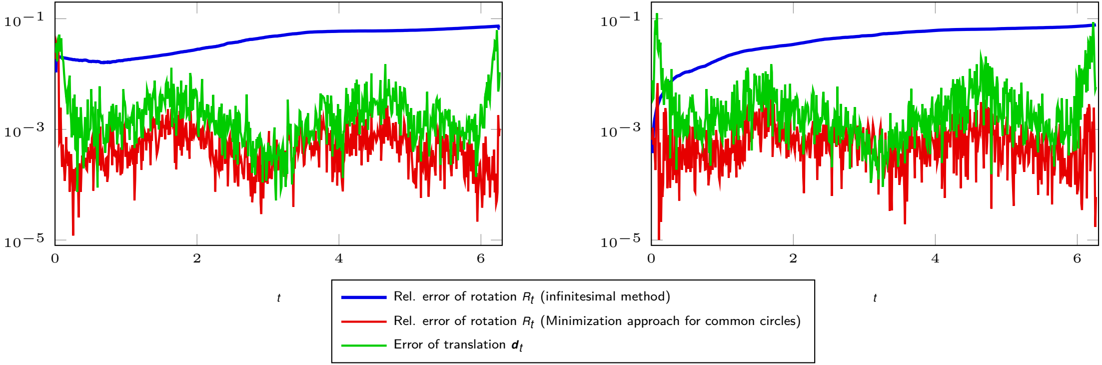

The rotation is around the moving axis $(\sqrt{1-a^2}\cos(b\sin(t/2)), \sqrt{1-a^2}\sin(b\sin(t/2)), a) \in \mathbb{S}^2$ for $a = 0.28$ and $b = 0.5$. The translation is $\boldsymbol{d}_t = 2(\sin t, \sin t, \sin t)$.
Left: cell phantom. Right: Shepp–Logan phantom.

Reconstructed Scattering Potential f

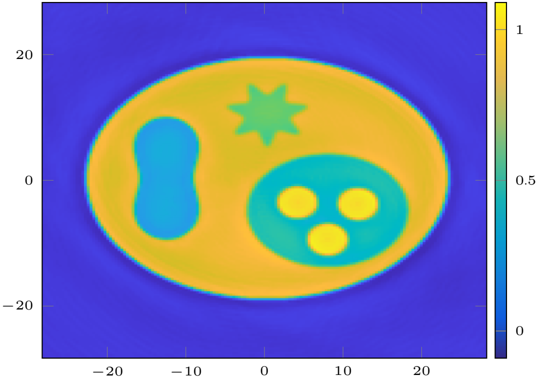

Cell phantom (PSNR 32.21, SSIM 0.754)

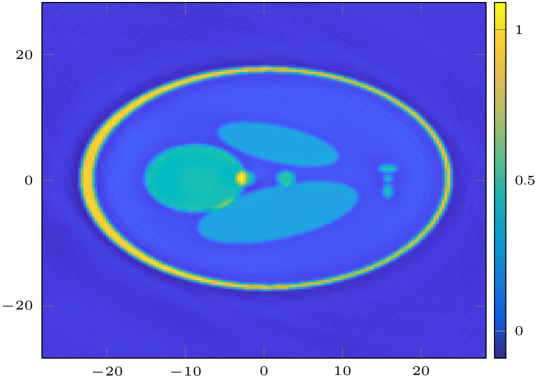

Shepp–Logan (PSNR 30.85, SSIM 0.772)

Conclusions

- Fourier diffraction theorem on $L^p(\mathcal{B}_{r_s})$, $p > 1$
- Backpropagation formula for arbitrary rotations
- Compared image reconstruction methods
  - Backpropagation is faster
  - Conjugate Gradients and Primal-Dual show better results
- Detection of rotation is usually possible
- Detection of translation is possible

Future research

- Application to real-world data
- Combining motion detection with phase retrieval

Thank you for your attention!

Conclusions

- Fourier diffraction theorem on $L^p(\mathcal{B}_{r_s})$, $p > 1$
- Backpropagation formula for arbitrary rotations
- Compared image reconstruction methods
  - Backpropagation is faster
  - Conjugate Gradients and Primal-Dual show better results
- Detection of rotation is usually possible
- Detection of translation is possible

Future research

- Application to real-world data
- Combining motion detection with phase retrieval

Thank you for your attention!

Conclusions

- Fourier diffraction theorem on $L^p(\mathcal{B}_{r_s})$, $p > 1$
- Backpropagation formula for arbitrary rotations
- Compared image reconstruction methods
  - Backpropagation is faster
  - Conjugate Gradients and Primal-Dual show better results
- Detection of rotation is usually possible
- Detection of translation is possible

Future research

- Application to real-world data
- Combining motion detection with phase retrieval

Thank you for your attention!